In situ spectroscopic ellipsometry analyses of hafnium diboride thin films deposited by single-source chemical vapor deposition

Yu Yang, Sreenivas Jayaraman, and Brent Sperling
Department of Materials Science and Engineering, University of Illinois at Urbana Champaign, 1304 West Green Street, Urbana, Illinois 61801 and Frederick Seitz Materials Research Laboratory, 104 South Goodwin Avenue, Urbana, Illinois 61801

Do Young Kim and Gregory S. Girolami
Department of Chemistry, University of Illinois at Urbana Champaign, 600 South Mathews Avenue, Urbana, Illinois 61801 and Frederick Seitz Materials Research Laboratory, 104 South Goodwin Avenue, Urbana, Illinois 61801

John R. Abelson[a]
Department of Materials Science and Engineering, University of Illinois at Urbana Champaign, 1304 West Green Street, Urbana, Illinois 61801 and Frederick Seitz Materials Research Laboratory, 104 South Goodwin Avenue, Urbana, Illinois 61801

(Received 31 July 2006; accepted 21 November 2006; published 4 January 2007)

In situ spectroscopic ellipsometry was used to analyze hafnium diboride thin films deposited by chemical vapor deposition from the single-source precursor $Hf(BH_4)_4$. By modeling the film optical constants with a Drude-Lorentz model, the film thickness, surface roughness, and electrical resistivity were measured *in situ*. The calculated resistivity for amorphous films deposited at low temperature ranged from 340 to 760 $\mu\Omega$ cm. These values are within 25% of those measured *ex situ* with a four-point probe, indicating the validity of the optical model. By modeling the real-time data in terms of film thickness and surface roughness, the film nucleation and growth morphology were determined as a function of substrate type, substrate temperature, and precursor pressure. The data show that at low precursor pressures ($\sim 10^{-6}$ Torr) and at low substrate temperatures (<300 °C), the onset of growth is delayed on both Si and SiO_2 surfaces due to the difficulty of nucleation. A higher substrate temperature or precursor pressure reduces this delay. At low temperatures the film morphology is a sensitive function of the precursor pressure because site-blocking effects change the reaction probability; the authors show that the morphology of newly grown film can be *reversibly* transformed from dense smooth to rough columnar by decreasing the precursor pressure. © *2007 American Vacuum Society.* [DOI: 10.1116/1.2409939]

I. INTRODUCTION

Transition metal diborides have attractive properties including extremely high melting temperatures, high thermal and electrical conductivities, high hardnesses, and high chemical stabilities.[1–3] Hafnium diboride (HfB_2), for example, has a melting temperature of 3250 °C and a bulk resistivity of 15 $\mu\Omega$ cm.[4] Owing to its remarkable properties, HfB_2 has potential applications in microelectronics: it performs well as a diffusion barrier between copper and silicon[5] and it has been investigated as a contact metal and a gate electrode material for Si metal-oxide-semiconductor field-effect transistors.[6,7]

In 1988, two groups independently discovered a highly attractive chemical vapor deposition route to HfB_2 thin films from the single-source precursor $Hf(BH_4)_4$.[8,9] We have recently shown that the kinetics of this chemical vapor deposition (CVD) process exhibits Langmuirian behavior, i.e., the reaction rate saturates at high precursor pressure.[10] Low temperature and high pressure conditions yield dense, smooth, homogeneous, and ultraconformal HfB_2 films. By varying the deposition conditions, we have also synthesized nanocrystalline hafnium diboride coatings and multilayer Hf–B–N composites that are extremely hard ($H \sim 40$ GPa).[11]

Spectroscopic ellipsometry (SE) is a powerful tool for characterizing thin films and studying thin film growth processes:[12–16] it measures the optical response of the material, including surface and substrate layers. When the electrical properties of the material are closely related to the optical properties, the former can be deduced,[17–19] and by applying appropriate models with consistent fitting parameters, SE affords accurate values for the film thickness, density, composition, and surface roughness. Because SE is an optical technique, the film growth process is undisturbed by the measurement, which allows for real-time, *in situ* analysis.

In this work, we use *in situ* SE to characterize the optical and electrical properties of hafnium diboride thin films grown by CVD from the single-source precursor $Hf(BH_4)_4$, and we analyze the nucleation, growth, and surface morphology evolution in real time. A Drude-Lorentz model provides an excellent estimate of the electrical resistivity. Effective medium theory shows that the surface morphology is a very strong function of the precursor sticking coefficient, which is modulated by changing the precursor pressure.

[a]Electronic mail: abelson@mrl.uiuc.edu

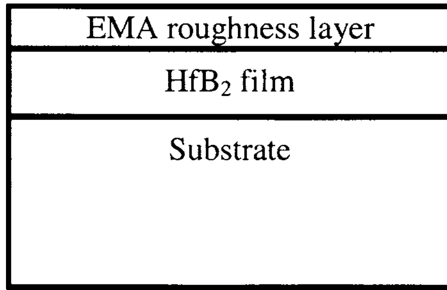

FIG. 1. Schematic diagram illustrating the different layers in the multilayer optical model used to fit the SE data.

II. EXPERIMENT

The HfB_2 films were deposited in an UHV system; the details of the reactor and growth process are described elsewhere.[5,10] In the present work, two types of HfB_2 films of interest for engineering applications were grown. Films grown at $200 \leqslant T \leqslant 350$ °C and at precursor pressures of $\geqslant 10^{-4}$ Torr are dense, conformal, x-ray amorphous, and morphologically homogeneous; films grown at 950 °C and very low precursor pressures of $\sim 10^{-6}$ Torr are heteroepitaxial and have physical properties close to those of bulk HfB_2. The low temperature HfB_2 films were grown on Si substrates or on Si covered with 100 nm of SiO_2; the SiO_2 overlayer was deposited by plasma enhanced CVD in a separate system. The higher temperature films were grown on Si(111) substrates. All substrates were ultrasonically cleaned in acetone, isopropyl alcohol, and de-ionized water before film growth. The silicon substrates were further dipped in a 10% HF solution to remove the native oxide before they were loaded into the growth chamber. The silicon surface is free of oxygen after the HF treatment, as verified by *in situ* Auger electron spectrometry which has a sensitivity of ~1% in monolayer surface coverage.

Film thicknesses were measured from scanning electron microscopy (SEM) images of fracture cross sections. The electrical resistivities of the films grown on SiO_2 were measured by the four-point probe method. The surface morphologies were analyzed by atomic force microscopy (AFM). *In situ* SE studies were carried out with a J.A. Woollam M-2000FI™ rotating compensator system with its accompanying software EASE™. The incident angle was fixed at 70°. The photon energies used for SE measurements spanned from the infrared to the ultraviolet (0.75–5.05 eV). For dynamic studies of growth, a spectroscopic scan was acquired every 2–10 s.

The SE data were modeled in terms of a multilayer model that includes a surface roughness layer, the film, and the substrate (Fig. 1). The analysis algorithm allowed the dielectric response of the film and the thicknesses of the film and roughness layer to vary in order to obtain a best fit to the data. The surface roughness layer was represented as an isotropic composite consisting of 50% void and 50% material using the Bruggeman effective medium approximation; this is a widely accepted procedure.[14,20] The dielectric constants of the HfB_2 film were modeled in terms of the Drude-Lorentz expression[21,22]

$$\varepsilon(E) = \varepsilon_{1\infty} - \frac{E_p^2}{E^2 + i\Gamma_D E} + \sum_{n=1}^{N} \frac{f_n E_n^2}{E_n^2 - E^2 - i\Gamma_n E}, \qquad (1)$$

where $\varepsilon_{1\infty}$ is a background term that compensates for the contribution of higher-energy transitions that are not taken into account by the Lorentz terms. The second term represents the free electron contribution described by the Drude model, where E_p is the unscreened plasma energy, Γ_D a damping factor due to electron scattering, and E the energy of the incident photon. The third term represents the contributions of interband transitions, modeled as damped Lorentz oscillators, where f_n, E_n, and Γ_n are the strength, center energy, and damping factors of the nth oscillator, respectively. For the CVD HfB_2 films, $\varepsilon_{1\infty}$ was fixed at 1.0 and two Lorentz oscillators were used in the model; therefore eight fitting parameters are required (E_p, Γ_0, f_1, E_1, Γ_1, f_2, E_2, and Γ_2). Extensive modeling showed that the use of only one Lorentz oscillator was insufficient to represent the optical data, suggesting that more than one interband transition is available. The optical resistivity (ρ_0) can be evaluated from the Drude term through the following expression:

$$\rho_0 = 7435 \frac{\Gamma_D}{E_p^2}, \qquad (2)$$

where Γ_D and E_p are in eV and ρ_0 is in $\mu\Omega$ cm.[22,23]

HfB_2 films with thickness $\geqslant 200$ nm are essentially opaque to the photon energies used here, and the SE data for such films are insensitive to the film thickness and the underlying substrate. To model such thick films, the film thickness was fixed to a value of >200 nm and the substrate was removed from the multilayer model. Regression analysis was performed to achieve a best fit between the model parameters and the experimental result, i.e., to minimize the mean square error (MSE) which is calculated from the difference in the experimental and model generated psi and delta values and weighted with respect to the experimental standard deviations at each wavelength.[24] In this work, we regard a fit with MSE $\leqslant 10$ to be a high quality fit and the corresponding model is reliable. For example, the excellent match between experimental and model generated data shown in Fig. 2 has a MSE value of 2.3.

III. RESULTS AND DISCUSSION

A. HfB_2 dielectric constants and resistivity

The single-source precursor $Hf(BH_4)_4$ was used to grow HfB_2 films to several different thicknesses for each process condition, and the films were examined by spectroscopic ellipsometry (SE). The HfB_2 films grown at 265–400 °C and $>10^{-4}$ Torr on SiO_2 substrates are amorphous, whereas the films grown at 950 °C and 10^{-6} Torr on Si(111) are heteroepitaxial. The SE data, taken in vacuum with the sample at room temperature, were fitted to the model described in Sec. II. Under the assumption that the film dielectric con-

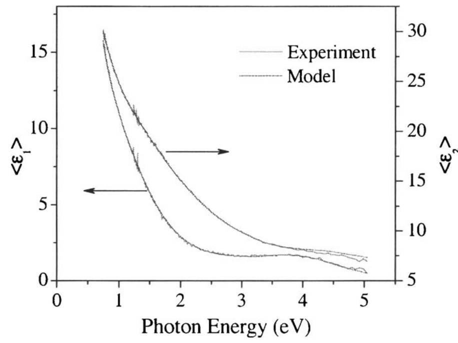

FIG. 2. Experimental and modeled $\langle \varepsilon_1 \rangle$ and $\langle \varepsilon_2 \rangle$ values vs photon energy for a HfB_2 film deposited on SiO_2 at 265 °C at 10^{-4} Torr. The MSE of this fit is 2.3.

stants are independent of thickness, we compared the film thickness extracted from the model with the thickness measured from cross sectional SEM micrographs; the modeled film thicknesses are within 5% of the SEM thicknesses. Table I lists the optical fitting results for the HfB_2 films grown under typical process conditions. Figure 2 shows the experimental and modeled pseudodielectric constants $\langle \varepsilon_1 \rangle$ and $\langle \varepsilon_1 \rangle$ versus photon energy for the amorphous film grown at 265 °C; the model fit is in excellent agreement with the data.

As judged from the best-fit parameters, the 265 and 300 °C films are very similar to each other, the 350 °C film is slightly different, and the 400 °C film and the 950 °C epitaxial film are drastically different. Optical differences can result from a number of factors including the film microstructure, stoichiometry, impurity content, crystallinity, or crystalline texture. In a previous study, we found that HfB_2 growth transits from reaction-limited to flux-limited CVD at ~350 °C.[10] Along with this kinetic transition, the film transforms from a homogeneous to a columnar structure and the mass density decreases from 70% to <50%.[5] This microstructural change reasonably explains the differences seen in the dielectric model for films grown at different temperatures in the 265–400 °C range. On the other hand, the epitaxial film grown at 950 °C is fully crystallized, highly oriented, and has a density close to the theoretical value.[5,25] It is not surprising that its optical constants are different from those of the amorphous films grown at lower temperatures. The

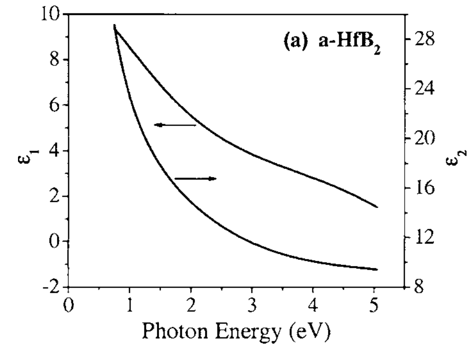

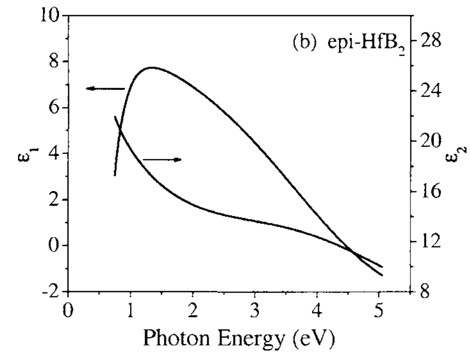

FIG. 3. Dielectric constants of HfB_2 obtained by fitting the SE data with the Drude-Lorentz model (a) for the amorphous film deposited on SiO_2 at 265 °C and $>10^{-4}$ Torr and (b) for the epitaxial film deposited on Si (111) at 950 °C and 10^{-6} Torr.

dielectric constants for the 265 °C amorphous film and for the epitaxial film, both deduced from the model, are shown in Fig. 3.

The last two columns of Table I compare, for each film, the optical resistivity calculated from Eq. (2) and the electrical resistivity measured by the four-point probe method. The directly measured resistivities are all greater than the optically calculated values by a factor of 1.3–1.4, except for the 400 °C film, for which the measured resistivity is higher by a factor of 3. The larger values observed for the directly measured resistivities probably arise because the four-point probe measurements were carried out *ex situ*: the HfB_2 films partially oxidize upon air exposure, which increases the film resistivity. The films grown at $T < 350$ °C are dense and homogeneous, and the oxidation is limited to a few nanometers

TABLE I. Drude-Lorentz parameters that produce a best fit to the ellipsometry data of the HfB_2 films grown by CVD from $Hf(BH_4)_4$ and resistivity calculated from the mode and resistivity measured by four-point probe.

Deposition temperature (°C)	Precursor pressure (Torr)	E_p (eV)	Γ_0 (eV)	E (eV)	f_1	Γ_1 (eV)	E_2 (eV)	f_2	Γ_2 (eV)	ρ_{calc} ($\mu\Omega$ cm)	ρ_{meas} ($\mu\Omega$ cm)
265	10^{-4}	13.0	8.8	2.5	5.7	4.7	6.6	5.6	7.2	390	510
300	10^{-4}	12.5	7.1	2.5	5.3	4.7	6.6	6.6	7.3	340	440
350	10^{-4}	6.8	4.7	2.3	1.9	2.9	6.3	4.2	7.1	760	1 080
400	10^{-4}	9.2	49.7	3.5	1.9	7.6	7.3	2.9	8.8	4380	14 100
950[a]	10^{-6}	3.3	0.1	2.5	28.3	9.6	4.9	8.4	6.8	98	15[b]

[a]An epitaxial film grown on Si(111) substrate.
[b]Bulk HfB_2 electrical conductivity.

near the film surface, as determined by the Auger electron spectrometry depth profiling. However, the 400 °C grown film has a low density columnar microstructure and oxidation occurs along the column boundaries.[5] This phenomenon presumably explains why the measured resistivity is a factor of 3 greater than the value calculated from the optical data. We could not measure the resistivity of the epitaxial HfB_2 film due to the parallel conduction of the silicon substrate. The optical resistivity (98 $\mu\Omega$ cm) is significantly smaller than for the amorphous films but is larger than the bulk HfB_2 value (15 $\mu\Omega$ cm). The epitaxial films are deposited at relatively low growth rates and are typically less than 20 nm thick; for films that are this thin, electron scattering at the film surface and interface are known to increase the resistivity above the bulk value.[26]

B. Film nucleation

Real-time ellipsometry was used to determine the onset of HfB_2 film growth. Owing to the large difference in optical constants between the metallic film and the dielectric substrate, as little as ~1 ML of film modifies the optical response; as a result, the first detectable change in optical response signals the onset of film growth. To measure the growth onset temperature, we held each substrate at a constant temperature for ~10 min and looked for a change in the ellipsometry signal; if no change occurred, the substrate temperature was increased by 25 °C and the 10 min examination period repeated. Under a low precursor pressure of 3×10^{-6} Torr, 300 °C is the minimum temperature for a HfB_2 film to grow on a clean Si or SiO_2 substrate. However, on a substrate already covered with a HfB_2 film, the growth onset temperature is only 200 °C at the same pressure, this difference implies that there is a larger nucleation barrier on the Si and SiO_2 surfaces relative to a HfB_2 surface. We have also detected this barrier in temperature programed reaction (TPR) studies.[10] At higher precursor pressures, the onset temperature decreases: for example, at a precursor pressure of $\geqslant 10^{-4}$ Torr, the onset temperature on clean Si or SiO_2 decreases to 200 °C.

We were able to obtain additional information about the nucleation rates from the observed incubation times at constant temperature, since these two parameters are inversely related.[23] For example, at 300 °C and a precursor pressure of 3×10^{-6} Torr, the incubation time is <1 min on a silicon substrate but is >4 min on a SiO_2 substrate. The nucleation rates are consistently fastest on HfB_2, slower on Si, and slower still on SiO_2. As a result, there is a range of parameters for which selective growth of a thin HfB_2 film on Si or metal, but not on SiO_2, can be achieved. The incubation time can be shortened by either increasing the precursor pressure or the growth temperature. These results are consistent with our earlier study using TPR methods.[10]

The evolution of the film growth, from nucleation to coalescence to steady-state film growth, can also be extracted from real-time SE measurements. An ellipsometry scan was taken every 2–10 s and subsequently fitted to the optical model described in Sec. II. We assume that the growing

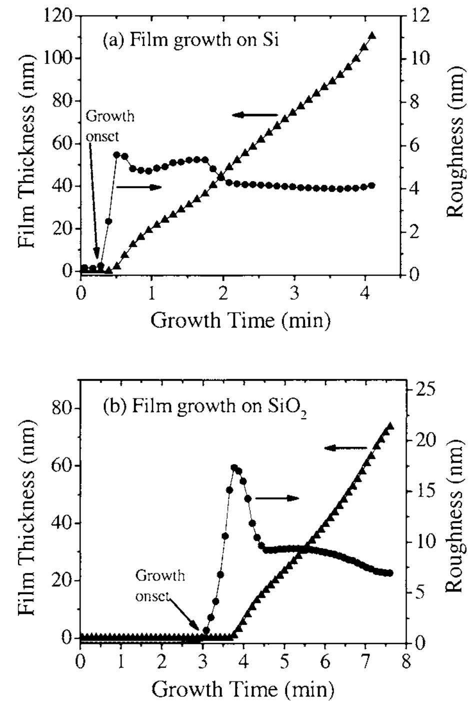

FIG. 4. Film thickness and surface roughness evolution with time determined by SE for HfB_2 deposition at 275 °C and 10^{-4} Torr on (a) a silicon substrate and (b) a SiO_2 substrate. The MSE values are less than 10 for all the fits, except for a few points near the peak roughness value.

HfB_2 film has the same Drude-Lorentz model parameters determined earlier; hence the only fitting parameters are the thicknesses of the film and of the surface roughness layer. For growth at 275 °C and 1×10^{-4} Torr, the thicknesses of the film and of the surface roughness layer evolve differently on Si [Fig. 4(a)] and SiO_2 [Fig. 4(b)] substrates. The incubation time is 3 min on SiO_2 but only 0.3 min on Si. The initial growth process can be divided into three stages: (1) nucleation, the rapid increase of the surface roughness while the nominal film thickness remains zero; (2) coalescence, the onset of the film thickening along with a decrease of the roughness; and (3) growth, the stabilization of the surface roughness and the linear increase of the film thickness. Growth on SiO_2 exhibits a much higher maximum roughness compared with the growth on Si; this high roughness suggests a low nucleation density, such that the nuclei grow taller before they coalesce. The high initial roughness cannot be fully eliminated during growth: the steady-state surface roughness is 7 nm on SiO_2 but only 4 nm on Si. SEM micrographs confirm that the film grown on SiO_2 is rougher (Fig. 5). Notably, the steady-state roughness can be reduced by using either a higher growth temperature or a higher precursor pressure to enhance the film nucleation.

Owing to the variable incubation time and the nonlinear growth rate during nucleation, it is difficult (from an engineering point of view) to grow ultrathin films with thicknesses of less than 100 nm based on the growth duration alone. To achieve a precise film thickness, real-time SE can be used to provide process control.

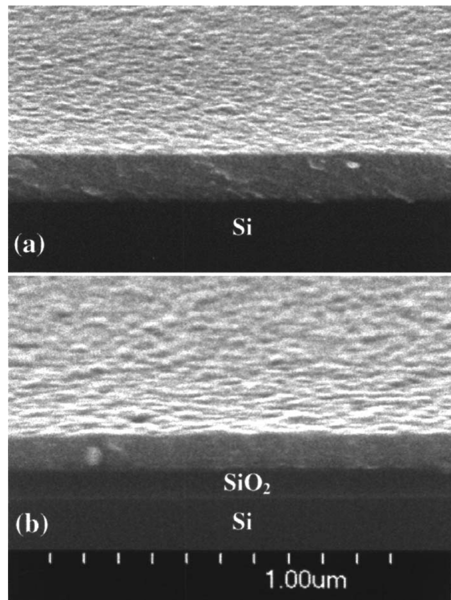

FIG. 5. SEM micrographs of HfB_2 films deposited at 275 °C and 10^{-4} Torr (a) on a silicon substrate and (b) on a SiO_2 substrate.

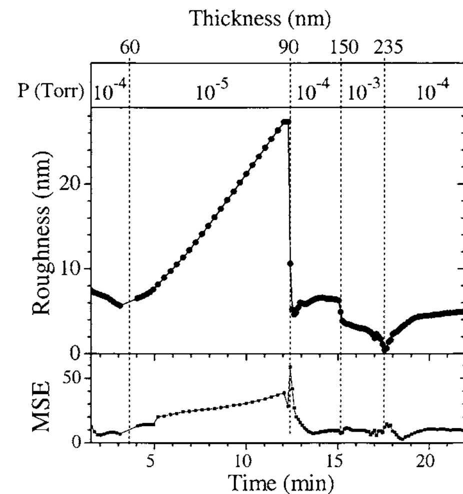

FIG. 6. Surface roughness evolution determined by SE for a HfB_2 film grown on Si at 275 °C with a $Hf(BH_4)_4$ precursor pressure sequentially stepped to 10^{-4}, 10^{-5}, 10^{-4}, 10^{-3}, and 10^{-4} Torr.

C. Growth morphology

The surface roughness of a thin film develops initially from the residual roughness of the nucleation and coalescence processes, as noted above. In general, the evolution of surface morphology is determined by the competition between roughening mechanisms such as self-shadowing that involve an instability and smoothing mechanisms such as surface diffusion or reemission that counteract the instability.[27] Here we use *in situ* SE to monitor the evolution of the surface roughness of the HfB_2 films as the pressure is changed with all other experimental variables held constant.

A HfB_2 film was grown at 275 °C on a Si substrate; the precursor pressure was varied between 10^{-5} and 10^{-3} Torr in discrete steps. The surface roughness (Fig. 6) shows a strong dependence on the pressure: at the higher pressures of 10^{-4} and 10^{-3} Torr, it is approximately constant at 6 and 3 nm, respectively. At the low pressure of 10^{-5} Torr, the roughness increases continuously with time and does not saturate. The MSE value at this pressure also increases with time, indicating that the fits become poor. Remarkably, when the pressure is increased from 10^{-5} to 10^{-4} Torr, the surface roughness decreases very rapidly, i.e., smoothing occurs.

To check the roughness value independently, films were grown at several precursor pressures in the range of 10^{-5}–10^{-3} Torr. SEM micrographs (Fig. 7) indicate that the surface is smoother when the pressure is higher, a finding that is consistent with the ellipsometry study. The film grown at 10^{-5} Torr has a columnar structure, whereas the films grown at higher pressures are dense and homogeneous. The inhomogeneity of the columnar microstructure explains the imprecise ellipsometry fits at 10^{-5} Torr. We also performed 1×1 μm^2 AFM scans; the corresponding rms roughness values of the films grown at 10^{-5}, 10^{-4}, and 10^{-3} Torr (Fig. 7) are 6.7, 3.0, and 1.3 nm, respectively. This trend is similar to that determined from the SE measurements, but the measured values are smaller than those determined optically (see above). The correlation between AFM and ellipsometrically determined roughness values involves a complicated function of the topography and is often nonlinear.[28,29] In the present case, the columnar structure of the films means that, due to tip convolution, AFM only scans the film surface and is not able to resolve deeper structure, whereas ellipsometry is more sensitive to the height and material density differences at the columnar boundaries. Although the ellipsometry fits are imperfect, the qualitative trends are significant.

The ellipsometry data demonstrate that the evolution of surface morphology results from a dynamic competition between roughening and smoothing mechanisms. The rougher surface of the films grown at low precursor pressures can be explained by the dependence of the precursor sticking coefficient on pressure. In a separate study, we showed that the surface reactions during growth from the $Hf(BH_4)_4$ precursor show a Langmuir adsorptionlike behavior,[10] such that the reactive sticking coefficient decreases as the precursor pressure is increased. It is well known that a high sticking coefficient leads to a rough surface and a columnar microstructure due to the self-shadowing effect.[30] In contrast, a low sticking coefficient leads to reemission of the adsorbed precursor molecule and smoothing of the surface because depressions on the surface receive more of the reemitted precursor flux than protrusions.[31] Depressions on the surface can also be regarded as microscopic trenches; we have shown elsewhere that high precursor pressures lead to extremely conformal coverage and eventual filling of trenches,[10] consistent with the smoothing of depressions observed here. The time required to fill a deep feature is roughly the time needed to grow a film with thickness comparable to the lateral dimension of the feature. Therefore it requires only seconds to smooth the surface roughness with a lateral dimension of nanometers, such as the gaps between columns of the film grown at 10^{-5} Torr.

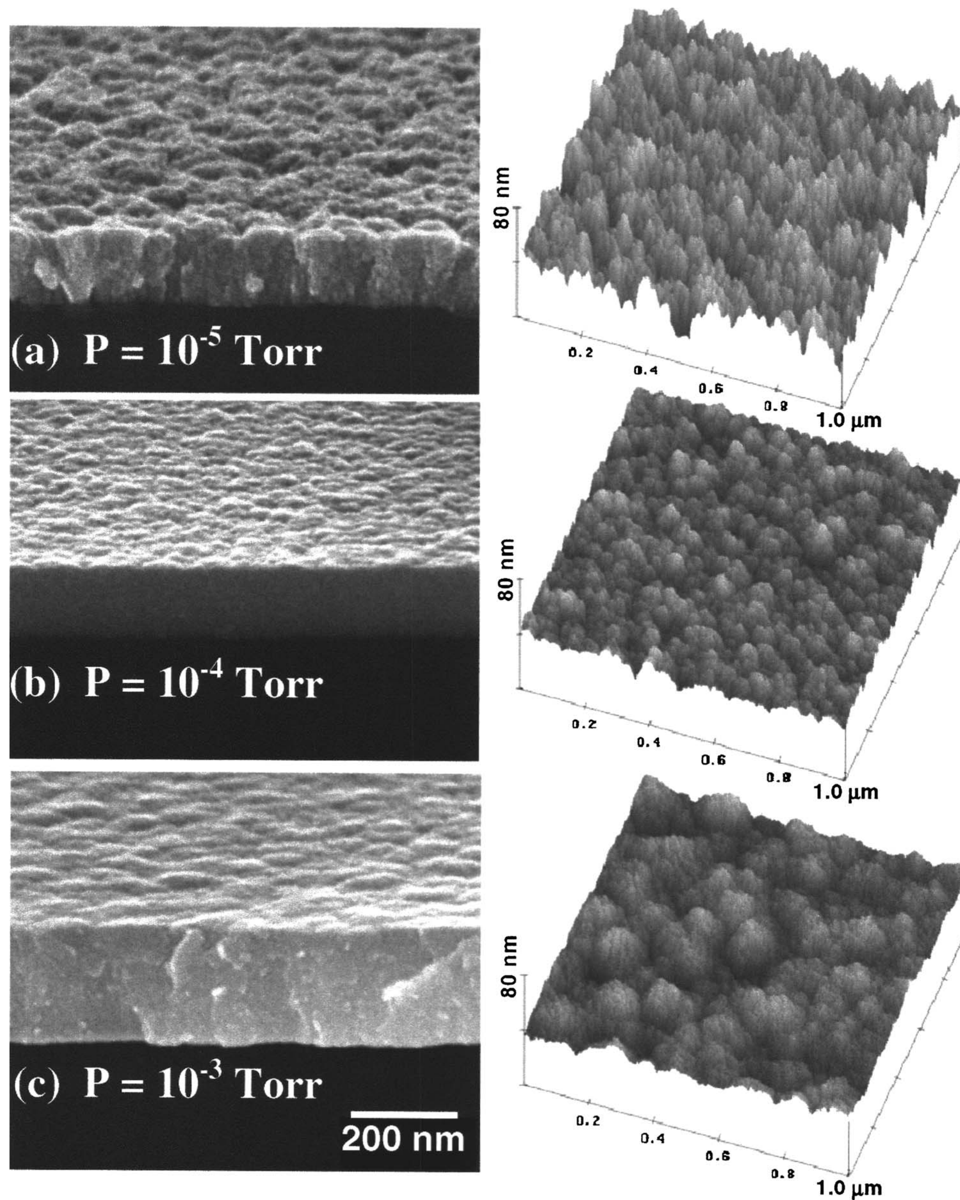

FIG. 7. SEM and AFM micrographs of HfB_2 films deposited on Si at 275 °C with precursor pressures of (a) 10^{-5} Torr, (b) 10^{-4} Torr, and (c) 10^{-3} Torr.

IV. CONCLUSIONS

Spectroscopic ellipsometry has been used to analyze the optical properties of hafnium diboride thin films grown by CVD from the single-source precursor $Hf(BH_4)_4$. The optical constants for amorphous HfB_2 and epitaxial HfB_2 films are evaluated from Drude-Lorentz models. For noncolumnar films, the model yields values for the electrical resistivity that are within 25% of those measured *ex situ* by a four-point probe. Real-time ellipsometry analysis of the growth process reveals a nucleation barrier on both Si and SiO_2 substrates that prevents film growth at $T<300$ °C when the precursor pressure is $<10^{-5}$ Torr. A longer incubation time and a higher roughness are observed on SiO_2 substrates in comparison with Si substrates, indicating that the nucleation rate is slower and the density of nuclei is lower on SiO_2. Ellipsometry measurements of the surface roughness reveal that a high growth pressure affords a smoother film and that the morphology can evolve *reversibly* between rough and smooth by modulating the precursor pressure between 10^{-5} and 10^{-3} Torr due to the strong reduction in reactive sticking coefficient with increasing pressure. The CVD of HfB_2 films appears very attractive for a variety of technological applications.

ACKNOWLEDGMENTS

The authors are grateful to the National Science Foundation for support of this research under Grant Nos. NSF CH-00-76061, NSF DMR-03-54060, and NSF DMR-03-15428. Compositional and structural analyses of the films were carried out in the Center for Microanalysis of Materials, University of Illinois, which is partially supported by the U.S. Department of Energy under Grant No. DEFG02-91-

ER45439. The authors also thank Leslie H. Allen at UIUC for the use of his four-point probe apparatus.

[1] *Properties and Uses of Diborides*, edited by J. Castaing and P. Costa (Springer, Berlin, 1977).
[2] C. Mitterer, J. Solid State Chem. **133**, 279 (1997).
[3] S. Motojima, K. Funahashi, and K. Kurosawa, Thin Solid Films **189**, 73 (1990).
[4] R. Kieffer and F. Benesovsky, *Hartstoffe* (Springer, Berlin, 1963).
[5] S. Jayaraman, Y. Yang, D. Y. Kim, G. S. Girolami, and J. R. Abelson, J. Vac. Sci. Technol. A **23**, 1619 (2005).
[6] W. Zagozdzon-Wosik *et al.*, Rev. Adv. Mater. Sci. **8**, 185 (2004).
[7] R. Ranjit, W. Zagozdzon-Wosik, I. Rusakova, P. van der Heide, Z. H. Zhang, J. Bennett, and D. Marton, Rev. Adv. Mater. Sci. **8**, 176 (2004).
[8] J. A. Jensen, J. E. Gozum, D. M. Pollina, and G. S. Girolami, J. Am. Chem. Soc. **110**, 1643 (1988).
[9] A. L. Wayda, L. F. Schneemeyer, and R. L. Opila, Appl. Phys. Lett. **53**, 361 (1988).
[10] Y. Yang, S. Jayaraman, D. Y. Kim, G. S. Girolami, and J. R. Abelson, Chem. Mater. **18**, 5088 (2006).
[11] S. Jayaraman *et al.*, Surf. Coat. Technol. **200**, 6629 (2006).
[12] R. W. Collins, J. Koh, H. Fujiwara, P. I. Rovira, A. S. Ferlauto, J. A. Zapien, C. R. Wronski, and R. Messier, Appl. Surf. Sci. **154**, 217 (2000).
[13] R. W. Collins, I. An, H. Fujiwara, J. C. Lee, Y. W. Lu, J. Y. Koh, and P. I. Rovira, Thin Solid Films **313**, 18 (1998).
[14] R. W. Collins, I. An, H. V. Nguyen, and T. Gu, Thin Solid Films **206**, 374 (1991).
[15] D. E. Aspnes, Proc. SPIE **452**, 60 (1984).
[16] J. N. Hilfiker, C. L. Bungay, R. A. Synowicki, T. E. Tiwald, C. M. Herzinger, B. Johs, G. K. Pribil, and J. A. Woollam, J. Vac. Sci. Technol. A **21**, 1103 (2003).
[17] P. Patsalas and S. Logothetidis, J. Appl. Phys. **90**, 4725 (2001).
[18] K. Postava, M. Aoyama, and T. Yamaguchi, Appl. Surf. Sci. **175**, 270 (2001).
[19] P. E. Schmid, M. S. Sunaga, and F. Levy, J. Vac. Sci. Technol. A **16**, 2870 (1998).
[20] I. An, Y. M. Li, H. V. Nguyen, and R. W. Collins, Rev. Sci. Instrum. **63**, 3842 (1992).
[21] H. G. Tompkins and W. A. McGahan, *Spectroscopic Ellipsometry and Reflectometry: A User's Guide* (Wiley, New York, 1999).
[22] R. E. Hummel, *Electronic Properties of Materials*, 2nd ed. (Springer, Berlin, 1992).
[23] J. Humlicek, A. Nebojsa, J. Hora, M. Strasky, J. Spousta, and T. Sikola, Thin Solid Films **332**, 25 (1998).
[24] The equation to calculate MSE is provided on J.A. Woollam website, http://www.jawoollam.com/Tutorial_6.html
[25] Y. Yang, S. Jayaraman, D. Y. Kim, G. S. Girolami, and J. R. Abelson, J. Cryst. Growth **294**, 389 (2006).
[26] G. Fishman and D. Calecki, Phys. Rev. Lett. **62**, 1302 (1989).
[27] D. G. Cahill, J. Vac. Sci. Technol. A **21**, S110 (2003).
[28] J. Koh, Y. W. Lu, C. R. Wronski, Y. L. Kuang, R. W. Collins, T. T. Tsong, and Y. E. Strausser, Appl. Phys. Lett. **69**, 1297 (1996).
[29] B. A. Sperling and J. R. Abelson, Appl. Phys. Lett. **85**, 3456 (2004).
[30] J. A. Thornton, J. Vac. Sci. Technol. A **4**, 3059 (1986).
[31] Y. P. Zhao, J. T. Drotar, G. C. Wang, and T. M. Lu, Phys. Rev. Lett. **8713**, 136102 (2001).